

Neutrino oscillations in strong gravitational fields

Dardo Píriz, Mou Roy, and José Wudka

Department of Physics, University of California, Riverside, California 92521-0413

(Received 8 December 1995; revised manuscript received 18 March 1996)

Neutrino oscillations in the presence of strong gravitational fields are studied. We look at very high energy neutrinos (~ 1 TeV) emanating from active galactic nuclei (AGN). It is observed that spin flavor resonant transitions of such neutrinos may occur in the vicinity of AGN due to *gravitational* effects and due to the presence of a large magnetic field (~ 1 T). A point to note is that matter effects (normal MSW transitions) become negligible in comparison to gravitational effects in our scenario. [S0556-2821(96)02914-1]

PACS number(s): 14.60.Pq, 04.62.+v

I. INTRODUCTION

It is well known that relativistic effects produce a precession of gyroscopes in the vicinity of a source of gravitational field [1]. It is, therefore, reasonable to expect that particles will undergo helicity flips in such regions. This is particularly interesting in the case of neutrinos, because left-handed neutrinos traversing a strong gravitational field could be converted into unobservable right-handed ones, resulting in a decrease of the neutrino flux.¹ We will analyze in this paper, following [3], the possibility of encountering resonant transitions of high energy Dirac neutrinos produced in active galactic nuclei (AGN) (reminiscent of the ones proposed as solutions of the solar neutrino problem [4–6]). The presence of such resonances alters the expectation of the neutrino flux on earth. In our calculations we will consider magnetic, matter, and gravitational effects. The latter are introduced using the standard couplings of neutrinos to gravity; we will not consider possible effects of the modification of the equivalence principle [7] in this paper.

The search for such high energy neutrinos by the neutrino telescopes [e.g., Deep Underground Muon and Neutrino Detector (DUMAND), Antarctic Muon and Neutrino Detector Array (AMANDA), (NESTOR), (BAIKAL), etc., [8]] which are under construction necessitates a clear picture of the expected neutrino fluxes from these objects. AGN are by far the strongest sources of ultrahigh energy neutrinos in the Universe, producing fluxes expected to be detectable on the earth with present technology [8]. These objects are believed to be fueled by the gravitational energy of matter accreting onto a supermassive black hole ($10^4 M_\odot$ to $10^{10} M_\odot$) at the AGN core, where gravitational energy is converted into luminous energy through the acceleration of high energy protons [9]. This environment exhibits copious production of hadronic and subsequent leptonic high energy by-products, such as neutrinos.

The paper is organized as follows. We start with a brief discussion of an AGN model and the mechanism of high energy neutrino production in it (Sec. II). In Sec. III we

study the possibility of neutrino transitions between different flavors and spins in the environment of a strong gravitational field using the semiclassical approximation. In Sec. IV we apply the formalism to the interesting case of a Kerr black hole; our main results are presented in this section. Finally, in Sec. V we give our conclusions. Several mathematical details are relegated to the Appendixes.

II. AGN MODEL

Active galactic nuclei have long been recognized as possible sources of high energy signals [10], being the most luminous objects in the Universe. They have luminosities ranging from 10^{42} to 10^{48} erg/sec, corresponding to black hole masses of the order of $10^4 M_\odot$ to $10^{10} M_\odot$, on the natural assumption that they are powered by Eddington-limited accretion onto the black hole. The spherical accretion model (based on works by Kazanas, Protheroe, and Ellison [11,12]) is used in most of the calculations of the neutrino production in central regions of AGN [9,13,14]. According to this scenario, close to the black hole the accretion flow becomes spherical and a shock is formed where the ram pressure of the accretion flow is balanced by the radiation pressure. We will follow this model even though it is only approximately true, considering that we will be looking at rotating black holes.

The distance from the AGN center to the shock, denoted as the shock radius \mathcal{R} (\approx a few Schwarzschild radii) contains the central engine of AGN. The shock radius is parametrized [11,12] by $\mathcal{R} = x r_g$, where r_g is the Schwarzschild radius of the black hole, and x is estimated to be in the range of 10 to 100 [9] (which is consistent with the available data [15]).

The matter density at the shock $\rho(\mathcal{R})$ can be estimated from the accretion rate needed to support black hole luminosity, and from the radius and accretion velocity at the shock [9],

$$\rho(\mathcal{R}) \approx 1.4 \times 10^{33} x^{-5/2} L_{\text{AGN}}^{-1} Q^{-1} \text{ g/cm}^3, \quad (1)$$

where $Q(x) = 1 - 0.1x^{0.31}$ is the efficiency for converting accretion power into accelerated particles at the shock [12], and L_{AGN} is the AGN continuum luminosity in units of erg/sec. In this model the matter density falls off as

¹Left-right transitions can occur as a gravitationally induced coherent precession, as investigated by Cai and Papini, [2]; it is in general quite small.

$$\rho_1(r) = \rho(\mathcal{R}) \left(\frac{r}{\mathcal{R}} \right)^{-3/2}, \quad r > \mathcal{R}. \quad (2)$$

Acceleration of protons is assumed to occur by the first-order diffusive Fermi mechanism at the shock [12]. Energy losses during acceleration occur through pp collisions in the gas;² and also through the $p\gamma \rightarrow p + e^+ + e^-$ and $p\gamma \rightarrow N\pi$ processes in the dense radiation fields present, mainly in the central region. All these reactions give rise to high energy neutrinos through the $\pi^\pm \rightarrow \mu^\pm \rightarrow e^\pm$ decay chain [9, 11, 16–18]. These neutrinos are expected to dominate the neutrino sky [9] at energies of 1 TeV and beyond.

Since neutrons are not confined by the magnetic field, they are free to escape from the central core [9]. But neutrons can also produce high energy neutrinos *via* np and $n\gamma$ collisions. The conclusion of Ref. [9] was that neutrons with energy less than approximately 10^3 TeV do escape the central core. On the other hand, Stecker *et al.* [19] found that secondary neutrons will not in general escape the shock radius, and argue that a significant amount of power is generated through $n\gamma$ interactions. However, according to them, confinement of nucleons in the central core occurs only for energies beyond $\sim 10^4$ TeV. In our study, as we shall see later, the matter density is irrelevant whatever the status of neutrons, confined or not.

Magnetic effects around AGN have important astrophysical consequences. To estimate a value of the magnetic field of AGN which we will use in our calculations, we look at two specific models. Both these models assume the ‘‘equipartition’’ condition that the external pressure is matched by the magnetic one. According to Begelman, Blandford, and Rees [20], a characteristic magnetic field B is given by

$$B = \frac{10^8}{(M/M_\odot)^{1/2}} \text{ G}, \quad (3)$$

where M is the mass of the black hole considered. Szabo and Protheroe [9] estimate the magnetic field at a shock formed by accretion to be

$$B \approx 5.5 \times 10^{27} Q^{-1/2} x^{-7/4} L_{\text{AGN}}^{-1/2} \text{ G}, \quad (4)$$

where the symbols have the same meaning as in Eq. (1). Since the shock is the site of high energy neutrino production, a good estimate of the value of magnetic field would be that evaluated at the shock. In the absence of a detailed model we will assume that the magnetic field remains approximately constant inside a region of size equal to the pressure scale height; the average fields of two of these regions will be uncorrelated. For $L_{\text{AGN}} = 10^{45}$ erg/sec, $M = 10^8 M_\odot$, and $x = 10$ both of the above expressions give $B \sim 10^4$ G. We will be interested in the vicinity of the horizon where the pressure scale height is $\sim r_g$. In this region we will assume that B remains at the above value. Outside the inner core of the AGN the magnetic field will drop as (pressure)^{1/2}.

²Accelerated protons interact with protons of the accreting plasma to form charged pions.

III. DIRAC EQUATION IN CURVED SPACE-TIME AND NEUTRINO OSCILLATIONS

We will study the possibility of neutrino oscillations between different flavors and spins in the environment of a strong gravitational field. In this paper we consider, for simplicity, the case of two family flavors only. We will also restrict ourselves to the case of Dirac neutrinos interacting minimally (as described by the equivalence principle) with the gravitational field.

The outline of our method to compute neutrino oscillations is the following. Starting with the Dirac equation in the presence of a strong gravitational field, we use a semiclassical expansion to different orders in the relevant parameters to determine the effective Hamiltonian for positive momentum states. We look in particular for the lowest order off-diagonal terms that could possibly induce gravitational neutrino oscillations, including the effects of magnetic fields associated with AGN. Once the Hamiltonian is obtained, we analyze the possibility of resonances depending on the neutrino mass, energy, and angular momentum, and the black hole mass and angular momentum. The different neutrino transitions and expected neutrino fluxes are then investigated.

A. Semiclassical approximation

We start with the Dirac equation in curved space-time [21],

$$[ie_a^\mu \gamma^a (\partial_\mu + \omega_\mu) - m + \mathbf{J}P_L] \psi = 0, \quad (5)$$

where e_a^μ are the tetrads, m is the mass matrix, \mathbf{J} is the weak interaction current matrix, P_L the left-handed projection operator, and the spin connection is

$$\omega_\mu = \frac{1}{8} [\gamma_a, \gamma_b] e^{va} e^b_{v\mu}, \quad (6)$$

where the semicolon denotes a covariant derivative; we use greek indices for coordinates in the general frame and roman indices for the local inertial frame. As in flat space, there are four neutrino states for each flavor that we separate into two states corresponding to neutrinos traveling towards or away from the observer. We call these *positive* and *negative* momentum states, respectively.

The first step in the semiclassical approximation is to replace the neutrino spinor by

$$\psi = e^{iS} \chi, \quad (7)$$

where S is the classical action defined in terms of the Lagrangian density $\mathcal{L}(x, \dot{x})$ and affine parameter l as

$$S = \int dl \mathcal{L}(x, \dot{x}), \quad \mathcal{L} = -\frac{1}{2} g_{\mu\nu} \dot{x}^\mu \dot{x}^\nu, \quad \dot{x} = \frac{dx}{dl} \quad (8)$$

(an overdot will always denote differentiation with respect to l), and solves the Hamilton-Jacobi equation

$$g^{\mu\nu}\partial_\mu S\partial_\nu S=0. \quad (9)$$

χ is constructed as the solution of the Hamilton-Jacobi equation and determines the trajectory of classical particles.

In order to proceed further we use the approach described by Sakita and Tsani [22]. If \bar{x} be the solution to the classical geodesic equation for massless particles, that is, the classical trajectory, a new set of local coordinates

$$\{l, \xi^A\}, \quad A=1,2,3 \quad (10)$$

is chosen such that

$$x^\mu = \bar{x}^\mu(l) + \nu_A^\mu(l)\xi^A. \quad (11)$$

Here $\nu_A^\mu(l)$ solves the variation equation

$$\partial_A \left\{ \left(\frac{\partial \mathcal{L}}{\partial x^\mu} \right) - \frac{d}{dl} \left(\frac{\partial \mathcal{L}}{\partial \dot{x}^\mu} \right) \right\}_{\xi=0} = 0 \quad (12)$$

to $O(\xi^2)$. The functions $\bar{x} + \nu_A \xi^A$ solve $\delta S=0$ to second order in ξ and so describe (approximately) a bundle of neighboring geodesics parametrized by the ξ^A ; the values of the ξ determine the separation of a given geodesic in the bundle from the reference geodesic $\bar{x}^\mu(l)$.

The semiclassical momentum is defined as

$$p_\mu = -\partial_\mu S|_{x=\bar{x}} \quad (13)$$

where the derivative is with respect to the end point. The solution to Eq. (9) is, to $O(\xi^2)$,

$$S = -p_\mu \nu_A^\mu \xi^A - \frac{1}{2} \left(\bar{\Gamma}_{\nu\rho}^\mu p_\mu \nu_A^\nu \nu_B^\rho + \frac{1}{2} \dot{N}_{AB} \right) \xi^A \xi^B, \quad (14)$$

where $\bar{\Gamma}_{\nu\rho}^\mu$ are the Christoffel symbols evaluated at $x=\bar{x}$, and

$$N_{AB} = \nu_A^\mu \nu_B^\nu g_{\mu\nu}. \quad (15)$$

From the geodesic equation obeyed by p^μ it follows that (see Appendix A)

$$p_\mu \nu_A^\mu = c_A = \text{const.} \quad (16)$$

In the following it will prove convenient to define a timelike vector p_\perp^μ which is the component of momentum p orthogonal to the ν_A^μ : namely,

$$p_\perp^\mu = p^\mu - c_A (N^{-1})^{AB} \nu_B^\mu. \quad (17)$$

B. Effective Hamiltonian

With the above preliminaries we are in a position to evaluate the effective Hamiltonian for the neutrino system. In order to make a systematic expansion let us define R to be the scale of the metric, so that, for example, $\omega_\mu \sim 1/R$; and let p be the order of magnitude of the momentum of the neutrinos. We imagine a localized wave packet of extension ξ propagating freely through a region of size R , where the gravitational field is essentially constant. The uncertainty relation requires that a change in the momentum is related to R via $\Delta p \sim 1/R$. This in turn implies that the angular spread of the wave packet is given by $\Delta\theta = \Delta p/p \sim 1/(pR)$, so that in a distance R a wave packet spreads $R\Delta\theta \sim 1/p$. But this spatial

spread is determined by the values of ξ for which the states are significantly different from zero, so that $\xi \sim 1/p$ [23].

Going back to the Dirac equation in curved space, Eq. (5), after substituting Eq. (7), we obtain the equation

$$(-e_a^\mu \gamma^a \partial_\mu S + i e_a^\mu \gamma^a \partial_\mu + \mathcal{V}_0 - m)\chi = 0, \quad (18)$$

where

$$\mathcal{V}_0 = i \gamma^a e_a^\mu \omega_\mu + \mathbf{J} P_L \quad (19)$$

and ω_μ is defined in Eq. (6).

We make a double expansion of χ , first in powers of ξ and then in powers of $1/pR$, as follows:

$$\chi = \chi^{(0)} + \chi_A^{(1)} \xi^A + O(\xi^2),$$

$$\chi^{(0)} = U_0 + U_{1/2} + U_1 + \dots; \quad U_\nu \sim (pR)^{-\nu}$$

$$\nu = 0, \frac{1}{2}, 1, \dots, \quad (20)$$

$$\chi_A^{(1)} = V_{1A} + V_{3A/2} + V_{2A} + \dots; \quad V_{\nu A} \sim R^{-1} (pR)^{1-\nu},$$

$$\nu = 1, \frac{3}{2}, 2, \dots$$

We substitute these expressions into the Dirac equation and make a double Taylor expansion in ξ and $1/(pR)$ and demand that each term vanish separately. In the perturbation we choose the mass to be $m \sim (p/R)^{1/2}$. This is for convenience in defining the perturbation expansion in an effort to look for the lowest order off-diagonal terms that might cause gravitationally induced helicity flips of neutrinos. For the lowest possible magnitude of the mass, i.e., $m \sim 1/R$, there are no off-diagonal terms in the Hamiltonian.

The result is the following set of mixed equations for the spinors $U_0, U_{1/2}, \dots$.

To $O(\xi^0)$,

$$\not{p} U_0 = 0, \quad \not{p} U_{1/2} = m U_0,$$

$$\not{p} U_1 + \frac{i}{p_\perp} \dot{U}_0 + i \mathbf{Y}^A V_{1A} + \bar{\mathcal{V}}_0 U_0 - m U_{1/2} = 0, \quad (21)$$

$$\not{p} U_{3/2} + \frac{1}{p_\perp} U_{1/2} + i \mathbf{Y}^A V_{3/2 A} + \bar{\mathcal{V}}_0 U_{1/2} - m U_1 = 0,$$

where

$$\mathbf{Y}^A = (N^{-1})^{AB} \left(\nu_{\mu B} - \frac{c_B p_\perp^\mu}{p_\perp} \right) \bar{e}_a^\mu \gamma^a \quad (22)$$

(the overbar represents variables evaluated on the geodesic: $x=\bar{x}$). To $O(\xi)$,

$$\not{p}V_{1A} = \chi_A U_0, \quad \not{p}V_{3/2A} = \lambda_A U_{1/2}, \quad (23)$$

where

$$\chi = \frac{1}{2} \dot{N}_{AB} \mathbf{Y}^B - \bar{e}_{a;v}^\mu p_{\mu} v_A^v \gamma^a. \quad (24)$$

From Eqs. (21) and (23) we obtain

$$\begin{aligned} i\dot{U}_0 &= \mathcal{O}U_0, \\ i\dot{U}_{1/2} &= \mathcal{O}U_{1/2} - \frac{im}{2} \mathbf{Y}^A V_{1A} - \frac{m}{2} \bar{V}_0 U_0 \end{aligned} \quad (25)$$

where

$$\mathcal{O} = -\frac{1}{2} \not{p} \bar{V}_0 + \frac{m^2}{2} - \frac{i}{2p_{\perp}} \not{p} + \frac{i}{2} \mathbf{Y}^A \chi_A. \quad (26)$$

It is now possible to reduce these equations to a Schrödinger-like equation (as shown in Appendix B) involving only χ , which reads

$$i\dot{\chi} = \left(\mathcal{O} - \frac{m}{2} \bar{V}_0 \right) \chi. \quad (27)$$

The above equation describes a set of states which are almost pairwise degenerate (due to the condition $\not{p}\chi=0$); the effective Hamiltonian \tilde{H}_{eff} for the positive momentum states is obtained using degenerate perturbation theory. Denoting by P_+ the projector onto the positive momentum states, we find

$$\tilde{H}_{\text{eff}} P_+ = P_+ \left(\mathcal{O} - \frac{m}{2} \bar{V}_0 \right) P_+. \quad (28)$$

It is always possible to go to the p_{\perp} rest frame where $p_{\perp}^a = E(1,0,0,0)$ and $p^a = E(1,0,0,1)$, neglecting the neutrino rest mass and using $p_{\perp}^2 = p \cdot p_{\perp}$; in this (local Lorentz) frame, the projector onto positive momentum states is

$$P_+ = \text{diag}(1,0,0,1). \quad (29)$$

In what follows we choose frames where the momentum has the form given above. In Appendix C we show that, with these previous considerations, Eqs. (27) and (28) lead to

$$\tilde{H}_{\text{eff}} = i\dot{\alpha} + \frac{1}{2} m^2 - p \cdot J_{\text{eff}} P_L + m \Theta^b \tau_b, \quad (30)$$

where $\dot{\alpha}$ is spin and flavor diagonal and has no observable consequences.³ The effective current is

$$J_{\text{eff}}^a = \bar{J}_W^a - \bar{J}_G^a. \quad (31)$$

Here \bar{J}_W^a is the weak interaction current, \bar{J}_G^a is defined as

$$J_G^a = \frac{1}{4} \epsilon^{abcd} \lambda_{fcd} \left(\eta_b^f + \frac{2p^f p_{\perp}^b}{p_{\perp}^2} \right), \quad (32)$$

and

³An imaginary contribution to α would signal a decrease in the overall neutrino flux and is also unobservable.

$$\lambda_{fcd} = (e_{f\mu,\nu} - e_{f\nu,\mu}) e_c^\mu e_d^\nu, \quad \eta^{ab} = \text{diag}(1, -1, -1, -1). \quad (33)$$

In order to determine \bar{J}_W^a we note that in the *rest frame of the accreting matter* it takes the form $J_{W;v_e}^0 = G_F(2N_p - N_n)/\sqrt{2}$ and $J_{W;v_e}^i = -G_F N_n/\sqrt{2}$, where G_F is the Fermi coupling constant and N_p and N_n are the proton and neutron number densities, respectively (only the zeroth component is nonvanishing in this frame). In the neutrino frame used above this becomes

$$J_{W;v_e}^a = \frac{G_F}{\sqrt{2}} (2N_p - N_n) u^a, \quad J_{W;v_e}^i = -\frac{G_F}{\sqrt{2}} N_n u^i, \quad (34)$$

where u^a denotes the four-velocity of matter in the chosen local inertial frame. In the model considered, matter is ultrarelativistic [11] (within the region of interest), so that $u^2 \approx 0$.

Finally,

$$\begin{aligned} \Theta^b &= \frac{1}{2} \bar{e}_{a;\mu}^\mu \epsilon^{acd} \frac{p_c p_{\perp d}}{p^2} + \frac{1}{2} \left(\bar{J}_W^a + \frac{1}{2} \epsilon^{acde} \bar{\gamma}_{cde} \right) \\ &\times \left(\eta_a^b + \frac{p_a p^b - p_{\perp a} p_{\perp}^b - p_a p_{\perp}^b}{p_{\perp}^2} \right). \end{aligned} \quad (35)$$

In addition to the gravitational effects it is essential to incorporate the effects of the magnetic field associated with AGN. It is well known that if a neutrino has nonvanishing magnetic moment (or transition magnetic moment of dipole type) μ_ν ,⁴ its helicity can be flipped when it passes through a region with a magnetic field which has a component perpendicular to the direction of motion. This idea has been analyzed by Okun and co-workers [24], and more recently the combined effects of flavor mixing, magnetic spin flip, and matter interactions have been considered [25,26]. The interaction with the electromagnetic field stems from a term of the form

$$\mu \sigma^{ab} F_{ab} \psi \quad (36)$$

(F_{ab} is the electromagnetic field tensor and $\sigma^{ab} = \frac{1}{4} [\gamma^a, \gamma^b]$) to be added to the left-hand side of Eq. (5); just as in the above references only the electric and magnetic fields in the direction orthogonal to p_{\perp} contribute. Denoting by E^r and B^r the components of the electric and magnetic fields, respectively, in the frame where $p^a = E(1,0,0,1)$, and using Eq. (36), we find that the effective Hamiltonian is modified according to

⁴Okun [24] pointed out that the manifestations of an electric dipole moment and magnetic dipole moment are practically indistinguishable for a highly relativistic neutrino. For simplicity, the term ‘‘magnetic moment’’ will be used in this paper to represent the combined effect of an electric and a magnetic dipole moment.

$$\tilde{H}_{\text{eff}} \rightarrow \tilde{H}_{\text{eff}} + \mu \sqrt{p_{\perp} \cdot p} \begin{pmatrix} 0 & \Omega^* \\ \Omega & 0 \end{pmatrix},$$

$$\Omega = (B^1 - E^2) + i(E^1 + B^2), \quad (37)$$

where μ denotes the magnetic moment matrix and B^a and E^a denote the magnetic and electric fields measured by a locally inertial observer.

We consider two generations with four-component Dirac neutrinos. Here we examine the ν_e - ν_{μ} system. The same can be done for the ν_e - ν_{τ} ν_{μ} - ν_{τ} systems. Using the chiral bases $\nu_{e_L}, \nu_{\mu_L}, \nu_{e_R}, \nu_{\mu_R}$, we can write the evolution equation for neutrino propagation through matter in the presence of a strong gravitational field as⁵

$$i \frac{d}{dl} \begin{pmatrix} \nu_{e_L} \\ \nu_{\mu_L} \\ \nu_{e_R} \\ \nu_{\mu_R} \end{pmatrix} = \tilde{H}_{\text{eff}} \begin{pmatrix} \nu_{e_L} \\ \nu_{\mu_L} \\ \nu_{e_R} \\ \nu_{\mu_R} \end{pmatrix} \quad (38)$$

where \tilde{H}_{eff} is the 4×4 matrix (30), containing the effects of the weak and gravitational interactions and the effects of electromagnetic field. An order of magnitude estimate (supported by explicit computations for particular metrics) shows that the Θ terms [Eq. (35), off-diagonal terms due to gravitational effects] in the effective Hamiltonian are negligible compared to the effects of the magnetic field for all interesting cases (see Sec. III D). The gravitational effects in the diagonal elements, however, are very relevant. The final expression for the effective Hamiltonian \tilde{H}_{eff} is

$$\tilde{H}_{\text{eff}} = \begin{pmatrix} -p \cdot J_{\text{eff}}^{\nu_e} + \frac{1}{2} \Delta m_{12}^2 \sin^2 \vartheta & \frac{1}{4} \Delta m_{12}^2 \sin 2\vartheta & E \mu_{ee} \Omega^* & E \mu_{e\mu} \Omega^* \\ \frac{1}{4} \Delta m_{12}^2 \sin 2\vartheta & -p \cdot J_{\text{eff}}^{\nu_{\mu}} + \frac{1}{2} \Delta m_{12}^2 \cos^2 \vartheta & E \mu_{\mu e} \Omega^* & E \mu_{\mu\mu} \Omega^* \\ E \mu_{ee} \Omega & E \mu_{e\mu} \Omega & 0 & 0 \\ E \mu_{\mu e} \Omega & E \mu_{\mu\mu} \Omega & 0 & \frac{1}{2} \Delta m_{12}^2 \end{pmatrix}, \quad (39)$$

where ϑ is the neutrino mixing angle, J_{eff} is given in Eq. (31), E is the energy of the particle, and Ω is defined in Eq. (37). Note that, because ν_{e_R} and ν_{μ_R} are sterile, i.e., do not interact electroweakly with matter, they can be considered vacuum mass eigenstates.

C. Resonances

Using Eq. (39) we can determine the AGN regions where resonant transitions occur [a phenomenon reminiscent of the Mikheyev-Smirnov-Wolfenstein (MSW) effect [4,6]]. These resonances are governed by the 2×2 submatrices of Eq. (39) for each pair of states.⁶

The five possible resonances are obtained by equating the diagonal terms for each submatrix and give rise to the resonance conditions

$$\frac{1}{2} \Delta m_{12}^2 \cos 2\vartheta + \sqrt{2} (p \cdot u) G_F N_p = 0 \quad (\nu_{e_L} \rightarrow \nu_{\mu_L}), \quad (40)$$

$$\frac{1}{2} \Delta m_{12}^2 \cos^2 \vartheta + \frac{p \cdot u}{\sqrt{2}} G_F N_n + p \cdot J_G = 0 \quad (\nu_{\mu_L} \rightarrow \nu_{e_R}), \quad (41)$$

$$-\frac{1}{2} \Delta m_{12}^2 \sin^2 \vartheta + \frac{(p \cdot u)}{\sqrt{2}} G_F N_n + p \cdot J_G = 0 \quad (\nu_{\mu_L} \rightarrow \nu_{\mu_R}), \quad (42)$$

$$\frac{1}{2} \Delta m_{12}^2 \cos^2 \vartheta + \frac{(p \cdot u)}{\sqrt{2}} G_F (2N_p - N_n) - p \cdot J_G = 0 \quad (\nu_{e_L} \rightarrow \nu_{\mu_R}), \quad (43)$$

$$-\frac{1}{2} \Delta m_{12}^2 \sin^2 \vartheta + \frac{p \cdot u}{\sqrt{2}} G_F (2N_p - N_n) - p \cdot J_G = 0 \quad (\nu_{e_L} \rightarrow \nu_{e_R}). \quad (44)$$

As will be shown in the following section the matter effects are very small compared to the gravitational effects, which makes J_G dominant whenever present [this makes irrelevant the precise value of N_n for the cases (41)–(44); only for the MSW resonance [4,6], Eq. (40), is the matter density important].

In order to determine whether the above resonances induce significant transition probabilities, we consider the corresponding 2×2 submatrices in detail. Each of these can, by a suitable subtraction from the diagonal term, be cast into the form

$$\begin{pmatrix} d & b \\ b & -d \end{pmatrix}, \quad (45)$$

where d is related to the matter and gravitational part and b to the magnetic field; their explicit form is

$$b = E \mu_{\nu} \Omega, \quad d = -p \cdot J_{\text{eff}} + (\Delta m^2 \text{ term}), \quad (46)$$

where E , μ_{ν} , and Ω are, respectively, the energy, magnetic moment of the neutrino, and electromagnetic field [see Eq.

⁵Note that the left-hand side involves differentiation with respect to the affine parameter which has units of E^{-2} , the units of length being E^{-1} . Therefore \tilde{H}_{eff} has units of E^2 , which differs from the usual units of the Hamiltonian.

⁶We will ignore multiple resonances which occur whenever three (or four) diagonal elements coincide; such resonances can occur only under very restricted circumstances.

(37)]; the “ Δm^2 term” depends on the specific 2×2 matrix and can be easily obtained from Eq. (39); it is always smaller than $|\Delta m_{12}^2|$.

Resonances occur when d vanishes, in which case the transition probability is well described (for sufficiently slowly varying d and b) by the Landau-Zener approximation [27]

$$P_{\text{LZ}} = \exp\left\{-2\pi^2 \frac{\beta^2}{\alpha}\right\}, \quad (47)$$

where

$$\beta = b|_{\text{res}}, \quad \alpha = \dot{d}|_{\text{res}}. \quad (48)$$

The condition for these resonances to induce an appreciable transition probability is

$$\beta^2 \geq \frac{\alpha}{2\pi^2}. \quad (49)$$

The presence of a magnetic field can also induce coherent precession of the states, which has been studied in sufficient detail in [24]. The condition for this to occur is, for slowly varying b and d in Eq. (45),

$$\frac{\sqrt{b^2 + d^2}}{E} R \geq 2\pi, \quad (50)$$

where R is the magnitude of the region where the magnetic field is coherent. In this case the transition probability is

$$P_{\text{prec}} \approx \frac{1}{2} \frac{b^2}{b^2 + d^2}, \quad (51)$$

which is significant when $b > d$. So, while the presence of a diagonal term requires a shorter distance R to generate rapidly varying phases, the very same effect decreases the transition probability: neutrino interactions with matter or gravitational effects effectively quench spin precession [28].

D. Estimates

The orders of magnitude for the weak and gravitational currents are, from Eqs. (34) and (32),

$$J_W = \frac{G_F \rho}{m_p} \sim 10^{-33} \rho \text{ eV}^{-1}, \quad J_G \sim R^{-1}, \quad (52)$$

where ρ is in units of eV^4 . According to Eqs. (1) and (2) the order of ρ for typical cases is $10^1 - 10^4 \text{ eV}^4$. Clearly, from above and taking $R \sim r_g$, the gravitational current part is found to dominate the weak current part for all relevant values of r_g (10^{14} to 10^{20} eV^{-1}).

The order of magnitude for the $m\Theta$ term in the Hamiltonian will be (considering that $\partial_\mu \sim R^{-1}$)

$$m\Theta^b \sim mR^{-1} \sim mr_g^{-1}. \quad (53)$$

If we compare this term with $E\mu_p\Omega$ for typical values ($E \sim 1 \text{ TeV}$, $\Omega \sim 10^4 \text{ G}$, $r_g \sim 10^{18} \text{ eV}^{-1}$), for a very small magnetic moment $\mu \sim 10^{-19} \mu_B$ and neutrino mass $m \sim 1 \text{ eV}$, we get

TABLE I. Approximate values for Δm^2 terms.

	$\Delta m_{12}^2 \cos^2 \vartheta \text{ (eV}^2\text{)}$	$\Delta m_{12}^2 \sin^2 \vartheta \text{ (eV}^2\text{)}$
Vacuum [29]	10^{-10}	10^{-11}
Solar small angle [29]	10^{-6}	10^{-8}
Solar large angle [29]	10^{-6}	10^{-6}
At. neutrinos [29]	10^{-3}	10^{-4}
LSND [30]	1	10^{-3}

$$\frac{E\mu\Omega}{m\Theta^b\tau_b} \sim 10^6. \quad (54)$$

Therefore, in what follows, we will neglect the Θ term.

The values for $|\Delta m_{12}^2|$ corresponding to different scenarios of neutrino oscillation are shown in Table 1.

The MSW resonances (40) correspond to

$$\Delta m_{12}^2 \sim 10^{-33} E \rho, \quad (55)$$

which, since $\rho \leq 10^4 \text{ eV}^4$ and $E \leq 10^{19} \text{ eV}$ (in order to get an appreciable flux) corresponds to $\Delta m^2 \leq 10^{-10} \text{ eV}^2$. Thus, aside from these extremely small values, *the usual MSW scenario does not take place.*

Since $p \sim E$, neglecting the weak current part,

$$p \cdot J_{\text{eff}} \sim \frac{E}{r_g}. \quad (56)$$

For a typical value of energy $E \sim 1 \text{ TeV}$, beyond which AGN neutrinos start dominating the sky, and $r_g \sim 10^{20} - 10^{14} \text{ eV}^{-1}$ ($M = 10^{10} M_\odot - 10^4 M_\odot$), $p \cdot J_{\text{eff}} \sim 10^{-8} - 10^{-2} \text{ eV}^2$. The orders of magnitude from Table I show that values of Δm^2 corresponding to the solar and atmospheric entries would undergo resonances in the vicinity of the black hole. Larger values of the mass difference [such as the Liquid Scintillation Neutrinos Detector (LSND) entry in the table] would resonate only at significantly larger energies (above 100 TeV); in order to have comparable resonance for atmospheric and LSND [30] values we need even more energetic neutrinos ($\sim 10^2$ and $\sim 10^6 \text{ TeV}$, respectively). A point to note here is that all resonant transitions do not occur simultaneously, as can be seen from Eqs. (40)–(44). At fixed conditions, for instance, the transitions ($\nu_{\mu_L} \rightarrow \nu_{e_R}$) and ($\nu_{e_L} \rightarrow \nu_{e_R}$) cannot both be realized together.

In order to determine whether the above resonances induce large transition amplitudes we will need to estimate the magnitude of Ω . The models we consider all assume that the magnetic field is determined by the “equipartition” condition [9] that the external pressure is matched by the magnetic one. The scale height for the pressure is $\sim r_g$ and so we expect the magnetic field to be uniform only through distances of order r_g ; on larger scales it will vary randomly. As we mentioned in Sec. I, the value of the magnetic field within these “coherence patches” is $|\Omega| \sim |B| \sim 10^4 \text{ G}$. Let us now define the scale height Λ for the effective current terms

$$\Lambda = \left| \frac{dl}{d(\ln p \cdot J_{\text{eff}})} \right|, \quad (57)$$

which has units of the affine parameter l . Then $\alpha \sim \Delta m^2/\Lambda$ and the condition (49) becomes

$$\mu_\nu \geq \frac{1}{EB} \left| \frac{\Delta m^2}{2\pi^2 \Lambda} \right|^{1/2} = \mu_{\text{min}}^{\text{res}}. \quad (58)$$

Resonant transitions will occur then if the relevant magnetic moment (or transition magnetic moment) satisfies this bound; this constraint depends, through Λ , on the type of metric and will be studied for some cases of interest in Sec. IV below. Note that we have assumed that the magnetic field remains constant over an interval of magnitude $\sim \Lambda$.

Within this estimate the condition for coherent precessions, Eq. (50), becomes

$$(\mu B r_g)^2 + \left(\frac{\Delta m^2 r_g}{E} + 1 \right)^2 > 4\pi^2 \quad (59)$$

and the transition probability (51) becomes large provided

$$\mu_\nu \geq \frac{1}{B r_g} \left(1 + \frac{\Delta m^2 r_g}{E} \right) = \mu_{\text{min}}^{\text{prec}}, \quad (60)$$

which is the condition for coherent precession to generate a significant number of helicity flips.

Comparing the different magnetic moment expressions obtained above, we get

$$\frac{\mu_{\text{min}}^{\text{prec}}}{\mu_{\text{min}}^{\text{res}}} = \left(\frac{\Delta m^2 r_g}{E} \right)^{1/2} + \left(\frac{\Delta m^2 r_g}{E} \right)^{-1/2}, \quad (61)$$

which implies $\mu_{\text{min}}^{\text{prec}} \geq 2\mu_{\text{min}}^{\text{res}}$ for any value of $\Delta m^2 r_g/E$.

Though realistic calculations would require an accurate profile for the magnetic field, the above results do provide useful order-of-magnitude estimates of the relevant quantities. We will use these expressions in Sec. IV B to estimate the possibility of transitions of each type.

IV. NEUTRINO OSCILLATIONS IN A KERR SPACE-TIME

In this section we will apply the formalism developed to the interesting case of a Kerr black hole.

A. Hamiltonian for the Kerr metric

The gravitational field of the rotating black hole is given by the following axially symmetric stationary Kerr metric [31]:

$$\begin{aligned} ds^2 = & \left(1 - \frac{r_g r}{\rho^2} \right) dt^2 - \frac{\rho^2}{\Delta} dr^2 - \rho^2 d\theta^2 \\ & - \left(r^2 + a^2 + \frac{r_g r a^2}{\rho^2} \sin^2 \theta \right) \sin^2 \theta d\phi^2 \\ & + \frac{2r_g r a}{\rho^2} \sin^2 \theta d\phi dt, \end{aligned} \quad (62)$$

where

$$\Delta = r^2 - r_g r + a^2, \quad \rho^2 = r^2 + a^2 \cos^2 \theta. \quad (63)$$

This metric depends on two constant parameters M and a , where M is the mass of the black hole and a is related to the angular momentum by the relation $L_{\text{BH}} = ma$; r_g is given by $r_g = 2M$ in geometrized units ($c = G = 1$). For $a = 0$ the Kerr metric becomes the Schwarzschild metric in the standard form.

We now consider the motion of a particle of mass m in a Kerr field.⁷ The Hamilton-Jacobi equation is fully separable in this case [32]. Writing the action S as

$$S = -Et + L\phi + S_r(r) + S_\theta(\theta), \quad (64)$$

where E is the energy and L the angular momentum of the particle, we obtain two ordinary differential equations

$$\left(\frac{dS_\theta}{d\theta} \right)^2 + \left(aE \sin\theta - \frac{L}{\sin\theta} \right)^2 + a^2 m^2 \cos^2 \theta = K, \quad (65)$$

$$\left(\frac{dS_r}{dr} \right)^2 - \frac{1}{\Delta} (r^2 E + a^2 E - aL)^2 + m^2 r^2 = -K, \quad (66)$$

where K is a new constant of motion. The four-momentum of the particle is then

$$p^a = \left(\gamma_0^{-1} E, \gamma_1^{-1} S'_r, \gamma_2^{-1} S'_\theta, \frac{L - g_{03} E / g_{00}}{k} \right) \quad (67)$$

where

$$\gamma_0 = \sqrt{g_{00}}, \quad \gamma_i = \sqrt{-g_{ii}}, \quad k^2 = \frac{g_{03}^2}{g_{33}} - g_{33}. \quad (68)$$

Our calculations involved a set of tetrads in which the momentum takes the form $p^a = E(1, 0, 0, 1)$. The corresponding tetrads are

$$e_\mu^a = \begin{pmatrix} \gamma_0 & 0 & 0 & \eta \\ 0 & \gamma_1 c_\alpha & 0 & k s_\alpha \\ 0 & -\gamma_1 s_\beta s_\alpha & \gamma_2 c_\beta & k s_\beta c_\alpha \\ 0 & -\gamma_1 c_\beta s_\alpha & -\gamma_2 s_\beta & k c_\beta c_\alpha \end{pmatrix},$$

where

$$s_\alpha = \sin\alpha, \quad c_\alpha = \cos\alpha, \quad (69)$$

and similarly for β ; α and β are the polar and azimuthal angles of p_a in Eq. (67). The angles satisfy the conditions

$$\tan\alpha = -\frac{p^1}{p^3}, \quad \tan\beta = -\frac{p^2}{\sqrt{(p^1)^2 + (p^3)^2}}. \quad (70)$$

Using the above relations we get an expression for the effective Hamiltonian for the Kerr metric (30). We use this to look at resonances in the next section. The explicit expres-

⁷Included only for completeness and to define the notation used later.

sion of the various terms in the Hamiltonian is quite involved (we include a brief description of such terms in Appendix D); here we present the results of numerical analysis of the expressions.

As a limiting case of the previous analysis, we consider the limit $a \rightarrow 0$, corresponding to a Schwarzschild black hole. The neutrino geodesics lie on a plane which we take as the $\theta = \pi/2$ plane. We then obtain $p_a \bar{J}_G^a = 0$ and the effective Hamiltonian reduces to

$$\tilde{H}_{\text{eff}} = \frac{1}{2} m^2 - \frac{E \bar{J}_W^{a=0}}{\sqrt{1-r_g/r}} \begin{pmatrix} 0 & 0 \\ 0 & 1 \end{pmatrix} + \mu \begin{pmatrix} 0 & \Omega^* \\ \Omega & 0 \end{pmatrix}, \quad (71)$$

where we assumed the absence of matter currents and where m and μ denote the mass and magnetic moment matrices, respectively. Thus, except for a factor $1/\sqrt{1-r_g/r}$ which is important only for $r \sim r_g$, the above expressions reduce to the flat-space situation. In particular, there is no gravitational contribution to the diagonal elements. One can also easily determine the off-diagonal terms Θ^b in Eq. (35), which give a contribution $mL\tau_2/(2Er^2)$ to \tilde{H}_{eff} (τ_2 denotes the usual Pauli matrix). As mentioned previously, these terms are negligible for all cases of interest due to the factor of m/E .

B. Resonances for the Kerr metric

We need to determine whether resonances are possible in the vicinity of a Kerr black hole. For a rotating black hole the spin flavor transition is due to the transference of orbital angular momentum to spin angular momentum and also due to the transference of the black hole's angular momentum to the neutrino spin. To determine possible resonant behavior, we will find the regions (r, θ) where each of Eqs. (40)–(44) is satisfied as a function of the parameters E, L, K, a , and r_g . We will do this for different values of Δm_{12}^2 and mixing angle. We choose normalized parameters

$$j = \frac{L}{Er_g}, \quad k = \frac{K}{(Er_g)^2} \quad (72)$$

for a neutrino obeying Eqs. (65) and (66). It is easy to see that $p \cdot J_{\text{eff}}$ can be written (neglecting the matter terms) in terms of the energy and Schwarzschild radius in the form

$$|p \cdot J_{\text{eff}}| = Er_g^{-1} f(r/r_g, \theta, j, k, a/r_g). \quad (73)$$

In Fig. 1 we show $\ln|f|$ as a function of (r, θ) , for an allowed value of the pair (j, k) , where an angular momentum ($a = 0.4r_g$) has been chosen for the black hole.⁸ $\ln|f|$ in Figs. 1, 4, and 5 represents the natural logarithm. We have plotted the magnitude of $p \cdot J_{\text{eff}}$ in an effort to give a clear picture of how resonances take place in this particular metric. It is to be borne in mind, however, that all resonance transitions do not occur simultaneously. Figure 2 presents the f contour plots under the same conditions as in Fig. 1.

⁸A realistic analysis of accretion onto black holes must account for the fact that the central hole is quite probably a Kerr black hole with angular momentum parameter a only slightly less than the gravitational mass [33].

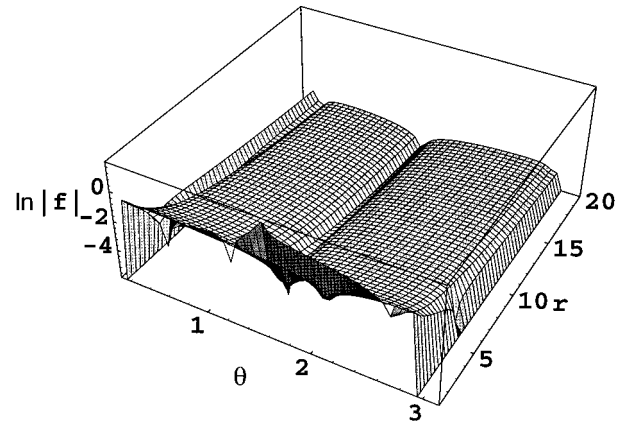


FIG. 1. Plot of $\ln|f|$ [see Eq. (73)] for the case $j=0.4$, $k=0.15$, $a/r_g=0.4$, and $M=10^8 M_\odot$.

Figure 3 illustrates the dependence of the function f for a specific value of (r, θ) on allowed values of (j, k) and taking $a = 0.4r_g$.

Resonances occur provided f is comparable to $\pm \Delta m_{12}^2 \cos^2 \vartheta r_g/E$ or $\pm \Delta m_{12}^2 \sin^2 \vartheta r_g/E$, as can be seen from Eqs. (41)–(44). As an example, we can analyze the case of energy $E \sim 1$ TeV, $r_g \sim 10^{18}$ eV⁻¹, and consider the solar large angle solution, $\Delta m_{12}^2 \sim 10^{-5}$ eV². Comparing this with f from Fig. 2, we find that it corresponds to contour a . We conclude then that resonances occur in the vicinity of the AGN for this choice of energies. In the same way it can be seen that resonances are present for all the given values of Δm^2 in Table I, all relevant black hole masses and angular momenta, and all neutrino energies above 1 TeV.

It is also of interest to determine the energy dependence of the resonance conditions, which is presented in Figs. 4 and 5.

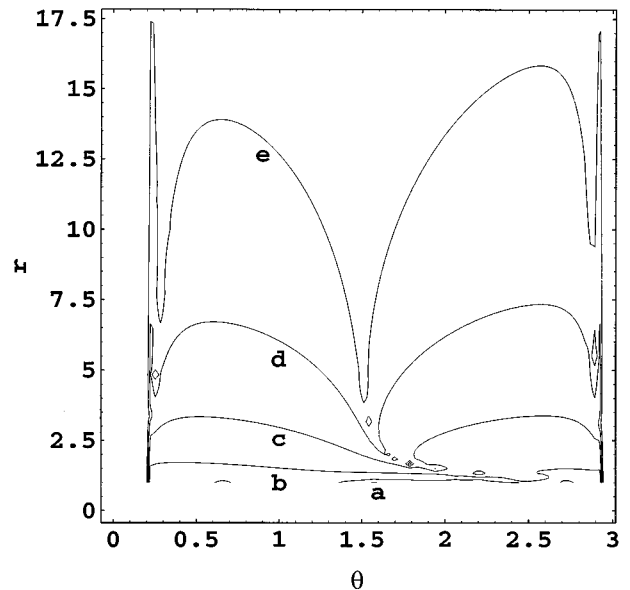


FIG. 2. Contour plot of f [see Eq. (73)] for $j=0.4$, $k=0.15$, $a/r_g=0.4$, and $M=10^8 M_\odot$. The contours a, b, c, d , and e correspond, respectively, to $f(a) = \pm 1$, $f(b) = \pm 10^{-1}$, $f(c) = \pm 10^{-2}$, $f(d) = \pm 10^{-3}$, and $f(e) = \pm 10^{-4}$, where positive values take place for $0 \leq \theta \leq \pi/2$, and negative ones for $\pi/2 \leq \theta \leq \pi$.

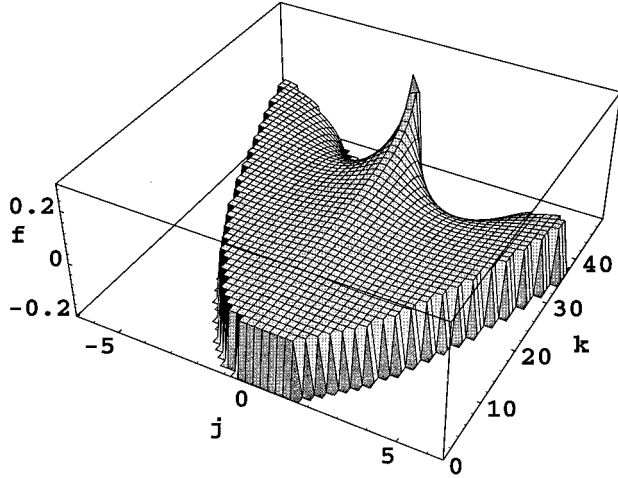


FIG. 3. Plot of f [see Eq. (73)] for $r=6r_g$, $\theta=\pi/2$, $a/r_g=0.4$, and $M=10^8 M_\odot$.

For fixed values of j, k, r and θ , the function f depends linearly on the energy E .

In order to determine the values of the magnetic moment which will allow for these resonances to induce large transition probabilities, we defined the quantity μ_{\min}^{res} in Eq. (58). This is plotted in Figs. 6 and 7 for some representative values of Δm^2 and E and for a magnetic field of 10^4 G.

The resonances which we described above will induce large transitions provided μ_ν is larger than μ_{\min}^{res} for the example considered this corresponds to $\sim(10^{-13}-10^{-14})\mu_B$ (where μ_B denotes the Bohr magneton). The above requirements lie comfortably inside the direct experimental bounds ($\mu_\nu \leq 10^{-10}\mu_B$) [34] as well as the astrophysical limits ($\mu_\nu \leq 10^{-11}\mu_B$) [34], and such values for the magnetic moment are consistent with a wide variety of models [35]. In view of this, the above resonances will induce significant transition probabilities whenever the resonance conditions (40)–(44) are satisfied.

The minimum of $\mu_{\min}^{\text{prec}}/\mu_{\min}^{\text{res}}$ in Eq. (61) [note that Eq. (61) involves only an order-of-magnitude calculation where $|f| \sim 1$, Eq. (73)] corresponds to $\Delta m^2 r_g/E \sim 1$, and then μ_{\min}^{prec} is comparable to μ_{\min}^{res} ; for $E=1$ TeV and $r_g \sim 10^{18}$ eV $^{-1}$ this

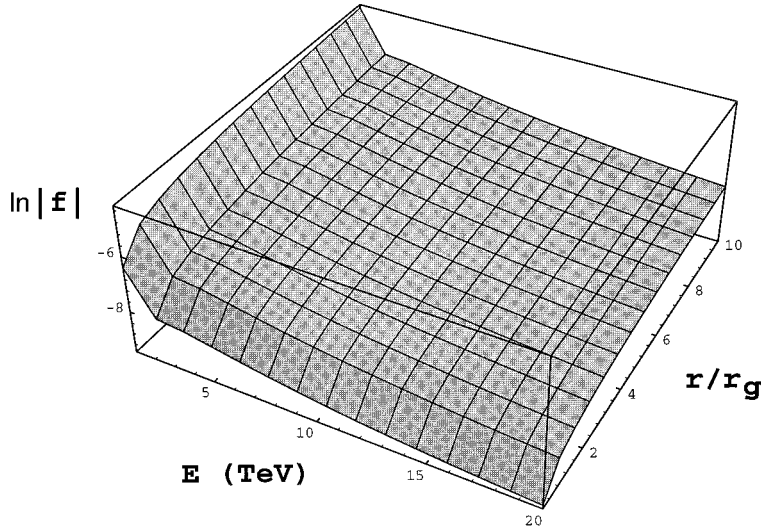


FIG. 4. Plot of $\ln|f|$ [see Eq. (73)] as a function of r and E for the case $\theta=\pi/4$, $j=0.4$, $k=0.15$, $a/r_g=0.4$, and $M=10^8 M_\odot$.

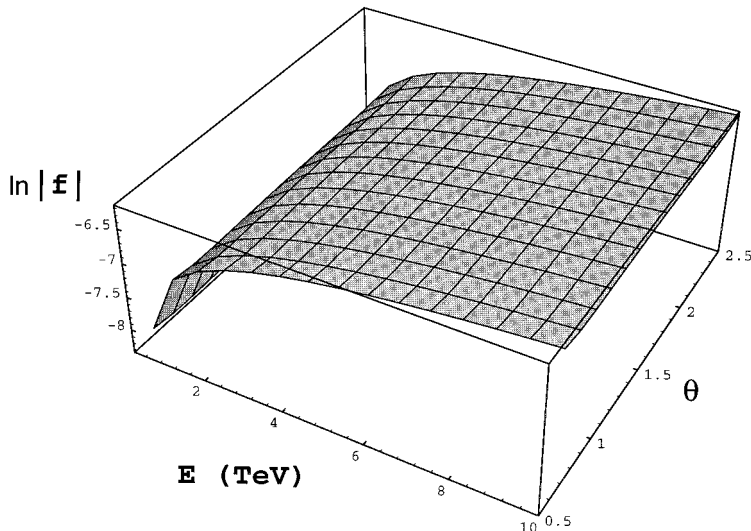


FIG. 5. Plot of $\ln|f|$ [see Eq. (73)] as a function of θ and E for the case $r=6r_g$, $j=0.4$, $k=0.15$, $a/r_g=0.4$, and $M=10^8 M_\odot$.

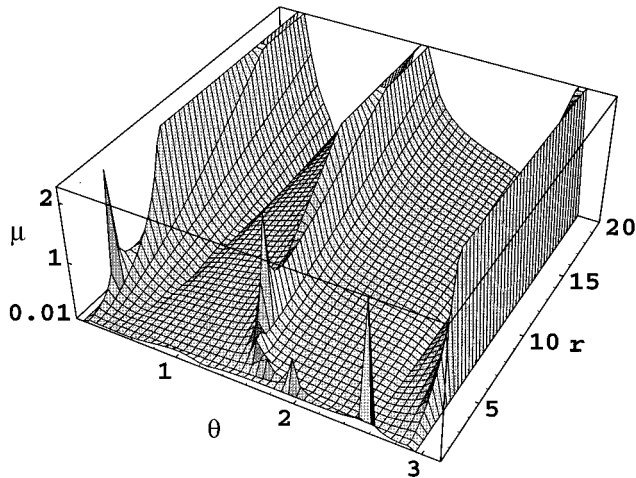


FIG. 6. Plot of $10^{13} \mu_{\min}^{\text{res}}$ [see Eq. (58)] for the case $\Delta m^2 = 10^{-6} \text{ eV}^2$, $E = 1 \text{ TeV}$, $j = 0.4$, $k = 0.15$, $a/r_g = 0.4$, and $M = 10^8 M_{\odot}$.

corresponds to $\Delta m^2 \sim 10^{-6} \text{ eV}^2$, which are the parameters used in Figs. 6 and 7. Explicit calculations show that $\mu_{\min}^{\text{prec}} > \mu_{\min}^{\text{res}}$ whenever $|f| > 1$, which at resonance corresponds to $\Delta m^2 r_g / E > 1$. The transition efficiency is greatest for the minimum value of the magnetic moment and corresponds to the spin flip in vacuum.

In order to estimate the effects of these resonances on the neutrino fluxes on Earth we note that neutrinos are expected to be generated mainly through the $\pi \rightarrow \mu \rightarrow e$ decay chain, implying that we can expect twice as many muon-type neutrinos as electron-type neutrinos. A negligible number of τ neutrinos are produced in an AGN environment. Even though the above calculations were done for the case of two species, we expect the same results for the case of three species: resonances will occur for all possible transitions. Such resonances will tend to “spill over” the neutrinos from the highly populated states into the less populated ones, evening out the neutrino numbers in all states. It follows that, with these simplistic assumptions, the muon-neutrino flux will be decreased by a factor of 1/4 and the electron neutrino

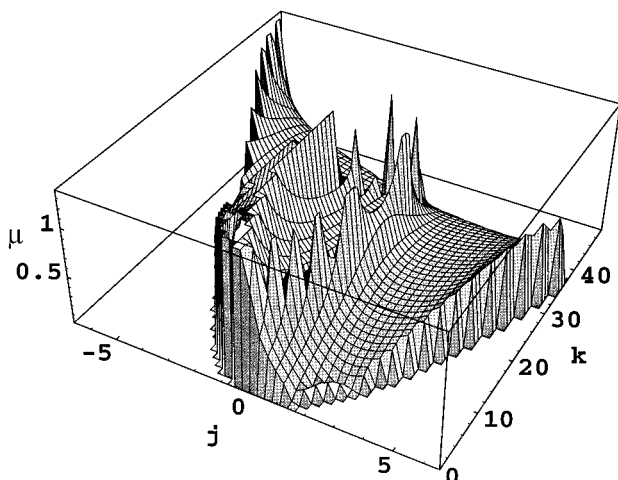


FIG. 7. Plot of $10^{13} \mu_{\min}^{\text{res}}$ [see Eq. (58)] for the case $\Delta m^2 = 10^{-6} \text{ eV}^2$, $E = 1 \text{ TeV}$, $r = 6r_g$, $\theta = \pi/2$, $a/r_g = 0.4$, and $M = 10^8 M_{\odot}$.

flux will decrease by a factor of 1/2, but we can expect as many τ neutrinos.

V. CONCLUSIONS

The evolution of neutrinos in an AGN environment is susceptible to gravity-induced resonances. Such resonances would induce various spin and spin flavor transitions whenever Eqs. (41)–(44) are satisfied. We have shown that such conditions would be expected to be satisfied for the currently accepted AGN models and for various neutrino parameters currently used in the literature.

Because of the lack of precise modeling of the AGN magnetic field (e.g., is the field dispersed or is it concentrated in flux tubes?), and lacking a better understanding of the parameters in the neutrino system, it is impossible to determine unambiguously whether such resonances would in fact occur in a given AGN.

Using the estimates for the magnetic fields, and approximating the gravitational field by the Kerr metric, the various values for Δm^2 we use do lead to resonances of the type (41)–(44). The corresponding transition probabilities will be large for a sufficiently large magnetic moment. Each resonance will occur at a different place along the neutrino trajectory; Figs. 1–3 show that essentially all neutrinos produced near the AGN core will traverse regions where all four resonance conditions are satisfied (for the neutrino parameters under consideration). Such resonances induce large transition probabilities for a wide variety of neutrino masses and energies (provided the neutrino magnetic moment is sufficiently large).

We do not expect resonant transitions to be 100% effective, whence the neutrinos will tend to populate all available states. Lacking detailed knowledge of the AGN environment, but relying on the fact that all resonances are viable, we can only estimate that all such states would end up by being equally populated. This, of course, depends on the masses of the neutrino states. For very small values of Δm^2 , $\Delta m^2 < 10^{-10} \text{ eV}^2$, Eq. (40) will be satisfied and MSW resonances will occur; the other possibilities (41)–(44) can be realized, but now farther from the AGN core where the estimate of the gravitational field is less reliable and where matter effects can no longer be ignored. We will not consider this (very complex) possibility further in this paper.

It is interesting to note that for $\Delta m^2 > 10^{-10} \text{ eV}^2$, the resonances described in this paper are not related to the MSW resonant flavor oscillations (which are suppressed in this environment due to the low densities present unless $\Delta m^2 < 10^{-10} \text{ eV}^2$; see Sec. III B), but to the interplay of the gravitational and electromagnetic interactions with the mass terms. Also, it must be noted that all resonance transitions do not occur simultaneously, as can be seen by studying Eqs. (40)–(44).

Noting that the AGN neutrinos travel through cosmological distances before being observed on Earth and taking the matter effects to be negligible on the way to the Earth, one might argue that the vacuum oscillations generated by the nonzero mass matrix would produce identical effects to the ones considered here. For a distance of approximately 100 Mpc (a sensible distance to AGN), vacuum oscillations occur for $\Delta m^2 < 10^{-19} \text{ eV}^2$ for 1 TeV energy neutrinos, which is

restrictively small. The effects of a cosmic magnetic field (the typical value of galactic [37] and galactic cluster [18] magnetic fields is of the order of 10^{-6} G; the intercluster magnetic field is $\leq 10^{-9}$ G [39]) can, of course, induce rapidly varying phases in the neutrino states, but the transition probability (51) is nonetheless small.

In our calculations we have chosen a rapidly rotating black hole ($a=0.4r_g$). This assumption is based on the conclusions of Ref. [33]. For lower values of a the conditions under which the resonances discussed in this paper can occur become more stringent. For the extreme limit of a Schwarzschild black hole, transitions are expected only in the immediate vicinity of the horizon.

In conclusion, we can say that gravitationally induced resonance transitions are the most important processes which can generate effective spin flavor conversion in active galactic nuclei. The precise expressions for the flux to be detected at Earth-bound neutrino telescopes depend, of course, on the details of the AGN model. We have shown, nonetheless, that for a very wide range of neutrino masses and even with very small magnetic moments, neutrinos will undergo resonant transitions. In their trip through the AGN environment the neutrinos can experience several such transitions, which tends to even out the population of all neutrino states. On one hand, this decreases the expected flux of electron and muon neutrinos; on the other hand, it dramatically increases the number of τ neutrinos of energies of 1 TeV and above. This provides strong motivation to search for such τ neutrinos with the existing neutrino telescopes, and the recently proposed 1 KM3 detector [36]. Even if the magnetic moments are $\sim 10^{-14} \mu_B$ we can expect an observable number of, for example, 10 TeV τ neutrino events; the precise number of such events is determined by the flux of electron neutrinos at that energy.

APPENDIX A

In this appendix we give a derivation of Eq. (16). Consider a geodesic $\bar{x}_\mu(l)$ for which the classical momentum is $\dot{\bar{x}}^\mu = p^\mu$ and solves the Hamilton-Jacobi equation $g_{\mu\nu} p^\mu p^\nu = 0$. Taking an l derivative we then obtain

$$2\dot{p}_\mu = \frac{\partial g_{\alpha\beta}}{\partial x^\mu} p^\alpha p^\beta. \quad (\text{A1})$$

Expanding x now to first order around the geodesic, $x^\mu = \bar{x}^\mu + \nu_A^\mu \xi^A$ [recall that this expression describes geodesics to $O(\xi^2)$] and substituting in the Hamilton-Jacobi equation yields

$$2\dot{p}_\mu \dot{\xi}^\mu + \frac{\partial g_{\alpha\beta}}{\partial x^\mu} p^\alpha p^\beta \xi^\mu = 0, \quad (\text{A2})$$

where $\xi^\mu = \nu_A^\mu \xi^A$. From Eqs. (A1) and (A2) it immediately follows that

$$0 = p_\mu \dot{\xi}^\mu + \dot{p}_\mu \xi^\mu = \frac{d}{dl} (p_\mu \xi^\mu). \quad (\text{A3})$$

Using the fact that the ξ^A are independent of l it follows that $p_\mu \nu_A^\mu = c_A = \text{const}$, as was to be shown.

APPENDIX B

In this appendix we show how to obtain a Schrödinger-like equation from Eq. (25). We note that

$$i\dot{U}_0 + i\dot{U}_{1/2} = \mathcal{O}(U_0 + U_{1/2}) - \frac{im}{2} \mathbf{Y}^A V_{1A} - \frac{m}{2} \bar{\mathcal{V}}_0 U_0. \quad (\text{B1})$$

But, from Eq. (20),

$$i\dot{U}_0 + i\dot{U}_{1/2} = i\dot{\chi} + O(1/R^2), \quad (\text{B2})$$

$$\frac{im}{2} \mathbf{Y}^A V_{1A} = \frac{im}{2} \mathbf{Y}^A \partial_A \chi + O(1/R^2),$$

and therefore by reordering terms in Eq. (B1)

$$i\left(\partial_l + \frac{m}{2} \mathbf{Y}^A \partial_A\right) \chi = \bar{\mathcal{O}} \chi + O(1/R^2), \quad (\text{B3})$$

where $\bar{\mathcal{O}}$ is given by

$$\bar{\mathcal{O}} = \mathcal{O} - \frac{m}{2} \bar{\mathcal{V}}_0. \quad (\text{B4})$$

The second term in Eq. (B3) describes the spreading of the wave packets and is not relevant for our discussion. We therefore ignore such terms. The final equation therefore reads

$$i\dot{\chi} = \bar{\mathcal{O}} \chi. \quad (\text{B5})$$

APPENDIX C

In this appendix we evaluate the effective Hamiltonian, given by Eq. (28), $H_{\text{eff}} P_+ = P_+ (\mathcal{O} - m \bar{\mathcal{V}}_0/2) P_+$, where \mathcal{O} and $\bar{\mathcal{V}}_0$ are defined in Eqs. (26) and (19). The explicit expressions are

$$\mathcal{O} = i\alpha + \frac{m^2}{2} - ip^a \bar{\gamma}_{abc} \sigma^{bc} - p_a \left(\bar{J}^a - \frac{1}{2} \epsilon^{abcd} \bar{\gamma}_{bcd} \right) P_L, \quad (\text{C1})$$

$$\bar{\mathcal{V}}_0 = \left(-\frac{i}{2} \gamma^{ba} \gamma_b + \frac{1}{2} \bar{J}^a \right) \gamma_a - \left(\frac{1}{4} \epsilon^{abcd} \bar{\gamma}_{bcd} + \frac{1}{2} \bar{J}^a \right) \gamma_a \gamma_5,$$

where

$$\bar{\gamma}_{abc} = \bar{e}_{ai;j} \bar{e}_b^i \bar{e}_c^j, \quad \sigma^{ab} = \frac{1}{4} [\gamma^a, \gamma^b]. \quad (\text{C2})$$

Using the explicit form of P_+ and working in the chiral representation for the gamma matrices we obtain

$$P_+ \gamma^a P_+ = i \epsilon^{abcd} \tau_b \otimes \tau^1 \frac{P_{\perp c} P_d}{P_{\perp}^2} P_+, \quad (\text{C3})$$

$$P_+ \gamma^a \gamma_5 P_+ = \left(-\eta^{ab} + \frac{p^a p_{\perp}^b + p_{\perp}^a p^b - p^a p^b}{P_{\perp}^2} \right) \tau_b \otimes \tau^1 P_+,$$

$$P_+ \sigma^{ab} P_+ = \frac{1}{2P_{\perp}^2} (p_{\perp}^a p^b - p_{\perp}^b p^a - i \epsilon^{abcd} p_c p_{\perp d} \gamma_5) P_+,$$

when $p^a = E(1,0,0,1)$ and $p_{\perp}^a = E(1,0,0,0)$. Using these relations we obtain

$$\tilde{H}_{\text{eff}} = i\dot{\alpha} + \frac{1}{2} m^2 - p \cdot J_{\text{eff}} P_L + m \Theta^b \tau_b, \quad (\text{C4})$$

where J_{eff} is given by Eq. (32) and Θ^b by Eq. (35).

APPENDIX D

In this appendix we show how to calculate the $p \cdot J$ term in the Hamiltonian; the metric is given in Sec. IV A. We will use the following notation:

$$\gamma_0 = \sqrt{g_{00}}, \quad \gamma_i = \sqrt{-g_{ii}}, \quad k^2 = \frac{g_{03}^2}{g_{33}} - g_{33}, \quad \eta = \frac{g_{03}}{\gamma_0}, \quad (\text{D1})$$

along with the tetrads

$$e_\mu^a = \begin{pmatrix} \gamma_0 & 0 & 0 & \eta \\ 0 & \gamma_1 c_\alpha & 0 & k s_\alpha \\ 0 & -\gamma_1 s_\beta s_\alpha & \gamma_2 c_\beta & k s_\beta c_\alpha \\ 0 & -\gamma_1 c_\beta s_\alpha & -\gamma_2 s_\beta & k c_\beta c_\alpha \end{pmatrix}, \quad (\text{D2})$$

$$e_{a\mu} = \eta_{ab} e_\mu^b,$$

and

$$e_a^\mu = \begin{pmatrix} \gamma_0^{-1} & 0 & 0 & 0 \\ -k \Xi c_\alpha s_\beta & \gamma_1^{-1} c_\beta & -\gamma_2^{-1} s_\alpha s_\beta & -k^{-1} c_\alpha s_\beta \\ -k \Xi s_\alpha & 0 & \gamma_2^{-1} c_\alpha & -k^{-1} s_\alpha \\ k \Xi c_\alpha c_\beta & \gamma_1^{-1} s_\beta & \gamma_2^{-1} s_\alpha c_\beta & k^{-1} c_\alpha c_\beta \end{pmatrix}$$

where

$$\Xi = g_{03}(g_{00}g_{33} - g_{03}^2)^{-1}. \quad (\text{D3})$$

With these expressions we construct λ_{abc} according to

$$\lambda_{abc} = (e_{a\mu, \nu} - e_{a\nu, \mu}) e_b^\mu e_c^\nu. \quad (\text{D4})$$

Explicitly,

$$p \cdot J = p \cdot (J_W + J_G), \quad (\text{D5})$$

where the currents are given in Eqs. (32) and (34), the weak current part being negligible compared to the gravitational part (as shown in Sec. III D), and

$$p \cdot J_G \approx \frac{1}{2} E (\lambda_{132} + \lambda_{213} + 3\lambda_{321} + 3\lambda_{021} + \lambda_{102} + \lambda_{210}), \quad (\text{D6})$$

where, for example,

$$\lambda_{132} = \left[\frac{s_\alpha s_\beta}{k^2 \gamma_1} (k - c_\alpha c_\beta \gamma_1^2) \partial_1 + \frac{c_\beta}{k^2 \gamma_2} (k s_\alpha^2 + \gamma_2^2 c_\alpha^2) \partial_2 + \frac{s_\alpha c_\alpha c_\beta}{k^2} (1 + k c_\beta) \partial_3 \right] k s_\beta. \quad (\text{D7})$$

The angles satisfy

$$\tan \alpha = -\frac{p^1}{p^3}, \quad \tan \beta = -\frac{p^2}{\sqrt{(p^1)^2 + (p^3)^2}}. \quad (\text{D8})$$

In the expression for λ_{abc} , ∂_i with $i=1,2,3$ represents ∂_r , ∂_θ , and ∂_ϕ , respectively. Similar expressions hold for the other values of λ_{abc} , which we will not list.

-
- [1] A. Papapetrou, Proc. R. Soc. London **A209**, 248 (1951); L. I. Schiff, Phys. Rev. Lett. **4**, 215 (1960); K. Sakina and J. Chiba, Lett. Nuovo Cimento **27**, 184 (1980).
- [2] Y. Q. Cai and G. Papini, Phys. Rev. Lett. **66**, 1259 (1991).
- [3] J. Wudka, in *High Energy Neutrino Astrophysics*, Proceedings of the Workshop, Honolulu, Hawaii, 1992, edited by V. J. Stenger *et al.* (World Scientific, Singapore, 1992).
- [4] L. Wolfenstein, Phys. Rev. D **17**, 2369 (1978).
- [5] J. N. Bahcall and H. Bethe, Phys. Rev. Lett. **65**, 2233 (1990).
- [6] S. P. Mikheev and A. Yu Smirnov, Yad. Fiz. **42**, 1441 (1985) [Sov. J. Nucl. Phys. **42**, 913 (1985)].
- [7] R. Colella *et al.*, Phys. Rev. Lett. **34**, 1472 (1975); L. M. Krauss and S. Tremaine, *ibid.* **60**, 176 (1988); J. M. Losecco, Phys. Rev. D **38**, 3313 (1988); S. Pakvasa *et al.*, *ibid.* **39**, 1761 (1989); A. Halprin *et al.*, *ibid.* **53**, 5365 (1996); H. Minakata and A. Smirnov, Report No. hep-ph/9601311, TMUP-HEL-9601, IC/96/9 (unpublished).
- [8] R. J. Wilkes, Proceedings of the SLAC Summer Institute, 1994 (to be published); H. W. Sobel, Nucl. Phys. B (Proc. Suppl.) **19**, 444 (1991); S. Barwick *et al.*, J. Phys. G **18**, 225 (1992); A. Roberts, Rev. Mod. Phys. **64**, 259 (1992).
- [9] A. P. Szabo and R. J. Protheroe, Astropart. Phys. **2**, 375 (1994).
- [10] V. S. Berezinsky, in *Neutrino 77*, Proceedings of the International Conference, Bakson Valley, USSR (Nauka, Moscow, 1977), Vol. 1, p. 177; D. Eichler, Astrophys. J. **232**, 106 (1979); R. Silberberg and M. M. Shapiro, in *Proceeding of the 16th International Cosmic Ray Conference*, Kyoto, Japan, 1979 (Institute for Cosmic Ray Research, Tokyo, 1979), Vol. 10, p. 357; V. S. Berezinsky and V. L. Ginzburg, Mon. Not. R. Astron. Soc. **194**, 3 (1981).
- [11] R. J. Protheroe and D. Kazanas, Astrophys. J. **265**, 620 (1983).
- [12] D. Kazanas and D. C. Ellison, Astrophys. J. **304**, 178 (1986).
- [13] M. C. Begelman, B. Rudak, and M. Sikora, Astrophys. J. **362**, 38 (1990).
- [14] M. Sikora and M. C. Begelman, in *High Energy Neutrino Astrophysics* [3].
- [15] A. Wandel and A. Yahil, Astrophys. J. **295**, L1 (1985).
- [16] D. Eichler, Astrophys. J. **232**, 106 (1979).
- [17] V. S. Berezinsky and V. L. Ginzburg, Mon. Not. R. Astron. Soc. **194**, 3 (1981).
- [18] M. Sikora *et al.*, Astrophys. J. **320**, L81 (1987).
- [19] F. W. Stecker, C. Done, M. H. Salamon, and P. Sommers, Phys. Rev. Lett. **66**, 2697 (1991); **69**, 2738(e) (1992).
- [20] M. C. Begelman, R. G. Blandford, and M. Rees, Rev. Mod. Phys. **56**, 255 (1984).
- [21] See, for example, B. S. DeWitt, *Dynamical Theory of Groups and Fields* (Gordon and Breach, New York, 1965).

- [22] B. Sakita and R. Tsani, in *Rationale of Beings, Festschrift in Honor of G. Takada*, edited by K. Ishikawa *et al.* (World Scientific, Singapore, 1985), pp. 283–290.
- [23] A similar procedure is described by J. Anandan, *Nuovo Cimento A* **53**, 221 (1979).
- [24] L. B. Okun, *Yad. Fiz.* **44**, 847 (1986) [*Sov. J. Nucl. Phys.* **44**, 546 (1986)]; L. B. Okun, M. B. Voloshin, and M. I. Vyotsky, *ibid.* **91**, 754 (1986) [*ibid.* **44**, 440 (1986)].
- [25] C. S. Lim and W. J. Marciano, *Phys. Rev. D* **37**, 1368 (1988).
- [26] E. Akhmedov and M. Khlopov, *Yad. Fiz.* **47**, 1079 (1988) [*Sov. J. Nucl. Phys.* **47**, 689 (1988)].
- [27] L. D. Landau, *Phys. Z. Sowjetunion* **1**, 426 (1932); C. Zenner, *Proc. R. Soc.* **A137**, 696 (1932).
- [28] M. Moretti, *Phys. Lett. B* **293**, 378 (1992).
- [29] See, for example, C. W. Kim and A. Pevsner, *Neutrinos in Physics and Astrophysics*, Contemporary Concepts in Physics Vol. 8 (Harwood Academic, Chur, Switzerland, 1993).
- [30] C. Athanassopoulos *et al.*, *Phys. Rev. Lett.* **75**, 2650 (1995).
- [31] L. D. Landau and E. M. Lifshitz, *The Classical Theory of Fields*, 4th ed. (Oxford, New York, 1975).
- [32] B. Carter, *Phys. Rev.* **174**, 1559 (1968).
- [33] S. L. Shapiro, *Astrophys. J.* **189**, 343 (1974).
- [34] Particle Data Group, L. Montanet *et al.*, *Phys. Rev. D* **50**, 1391 (1994).
- [35] M. B. Voloshin, *Yad. Fiz.* **48**, 804 (1988) [*Sov. J. Nucl. Phys.* **48**, 512 (1988)]; R. Barbieri and R. N. Mohapatra, *Phys. Lett. B* **218**, 225 (1989); K. S. Babu and R. N. Mohapatra, *Phys. Rev. Lett.* **64**, 1705 (1990); G. Ecker, W. Grimus, and H. Neufeld, *Phys. Lett. B* **232**, 217 (1989).
- [36] J. G. Learned and S. Pakvasa, *Astropart. Phys.* **3**, 267 (1995); S. Pakvasa, in *Beyond the Standard Model IV*, Proceedings of the International Conference, Lake Tahoe, California, edited by J. Gunion *et al.* (World Scientific, Singapore, 1995), Report No. hep-ph/9503369 (unpublished).
- [37] E. N. Parker, *Cosmical Magnetic Fields* (Oxford University Press, Oxford, 1979), and references therein.
- [38] A. R. Crusius-Wätzel *et al.*, *Astrophys. J.* **360**, 417 (1990); K. T. Kim *et al.*, *ibid.* **379**, 80 (1990); D. Sokolov *et al.*, *Astron. Astrophys.* **264**, 396 (1992).
- [39] E. R. Harrison, *Mon. Not. R. Astron. Soc.* **165**, 185 (1973); E. G. Zweibel, *Astrophys. J.* **328**, L7 (1988).